Available online at www.sciencedirect.com

SciVerse ScienceDirect

Ceramics International 38 (2012) 2421–2427

CERAMICS INTERNATIONAL

www.elsevier.com/locate/ceramint

Dielectric, electromagnetic absorption and interference shielding properties of porous yttria-stabilized zirconia/silicon carbide composites

Xiaowei Yin *, Yeye Xue, Litong Zhang, Laifei Cheng

National Key Laboratory of Thermostructure Composite Materials, Northwestern Polytechnical University, P.O. Box 547, Xi'an, Shaanxi 710072, PR China

Received 25 July 2011; received in revised form 11 October 2011; accepted 3 November 2011
Available online 9 November 2011

Abstract

SiC was infiltrated into porous yttria-stabilized zirconia (YSZ) felt by chemical vapor infiltration (CVI), and continuous SiC matrix layer was formed around YSZ fibre. When 86.9 wt.% SiC is introduced into the porous YSZ felt, the mean values of the real part of the permittivity and dielectric loss tangent of porous YSZ felt increase from 1.16 and 0.007 to 8.2 and 1.31, respectively. The electromagnetic interference (EMI) shielding efficiency (SE) increases from 0.069 dB to 16.2 dB over the frequencies ranging from 8.2 GHz to 12.4 GHz. The reflection loss of the composites with a thickness of 5 mm at 8–18 GHz is smaller than −6.5 dB, and the bandwidth below −10 dB is 5 GHz at room temperature, which increases to 5.9 GHz at 800 °C. The considerable increases in EMI SE and microwave absorption properties are attributed to the formation of continuous SiC matrix layer composed of SiC nanocrystals in the porous YSZ felt, which is beneficial for the production of induced electric current and the enhancement of dielectric loss.

Keywords: B. Fibres; B. Composites; C. Dielectric properties; D. SiC; D. ZrO_2

1. Introduction

Materials used for electromagnetic interference (EMI) shielding and electromagnetic (EM) wave absorbing are attracting worldwide attentions for the purpose of protecting the workspace and the environment from the radiation emitted by telecommunication apparatus [1]. Ceramics and its composites exhibit potential as EM wave shielding and absorbing materials [2–8], which can be used in corrosive environments at high temperature. SiC is a group IV polar semiconductor, having a wide band gap, and has many practical and potential applications in EM wave absorption [9,10]. The dielectric properties and microwave absorbing properties of various SiC including SiC powders [11], SiC nanofiber [12], SiC foams [13], and SiC matrix composites [14] have been investigated. Recently, the high-temperature microwave absorbing properties of carbon materials [15], MnO_2 nanorods [16], ZnO [17], and carbon nanotube [18], etc. have been widely explored. However, little literature on the microwave absorption properties of the SiC-based materials at high temperature is reported, as well as the EMI shielding properties.

Yttria stabilized-zirconia (YSZ) has good physical and chemical properties such as high chemical, thermal, and mechanical stability [19,20]. Composites consisting of mixtures of SiC dispersed within an YSZ host may exhibit a controllable variation in relative complex permittivity by adjusting the material composition during synthesis [21,22].

In the present work, YSZ fibre felts were used as preform, which were infiltrated with SiC by chemical vapor infiltration (CVI) to fabricate porous YSZ/SiC composites. CVI method has various advantages: (1) the process can be conducted at low pressure and low temperature, no external pressure is required, so fibre reinforced ceramic matrix composites with high performance can be fabricated owing to the small residual stress and less damage of the fibre; (2) the phase composition of the matrix can be easily designed by adjusting the kind, concentration, and deposition sequence of the reaction gases; (3) components with complex shape and high volume content of fibres can be fabricated by a near-net shape process. The effects of SiC content in porous YSZ/SiC composites on dielectric properties and EMI shielding properties were studied. Microwave absorbing

* Corresponding author. Tel.: +86 29 88494947; fax: +86 29 88494620.
E-mail address: yinxw@nwpu.edu.cn (X. Yin).

0272-8842/$36.00
doi:10.1016/j.ceramint.2011.11.008

properties were measured at temperatures ranging from room temperature to 800 °C.

2. Experimental procedures

2.1. Materials preparation and microstructure characterization

Porous YSZ short fibre felt with average diameter of 7 μm and density of 0.04 g/cm^3 was denoted as sample A. SiC matrix was infiltrated into sample A using methyltrichlorosilane (MTS, $CH_3SiCl_3 \geq 98.0$ wt.%) as precursor by low pressure CVI. Hydrogen ($H_2 \geq 99.99\%$) acted as carrier gas of MTS and argon (Ar $\geq 99.9\%$) as dilution gas with a MTS/H_2 ratio of 1/10 at 3 kPa. After CVI for 80–320 h at 1000 °C, SiC content increased from 86.9 to 97.9 wt.% with density of porous YSZ/SiC composites varying from 0.34 to 2.18 g/cm^3, which were denoted as samples B, C, D and E in Table 1.

The phase composition was measured by X-ray diffraction (XRD, X'pert PRO, Philips, Netherlands) with Cu Kα radiation. The microstructure of the samples was observed by a scanning electron microscopy (SEM, S-4700, Hitachi, Japan). Density and open porosity of the samples were measured by Archimedes method according to ASTM C-20 standard.

2.2. Measurement of dielectric property and valuation of EMI shielding property

The relative complex permittivity ($\varepsilon = \varepsilon' - j\varepsilon''$) with the real part of the permittivity ε' and the imaginary part ε'' of samples (22.85 mm × 10.15 mm × 3 mm) was measured on a vector network analyzer (VNA) (MS4644A, Anritsu, Japan) over the frequencies ranging from 8.2 GHz to 12.4 GHz (X-band) using wave-guide method.

After the dielectric measurement, the scattering parameters (*S*-parameters) that correspond to the reflection (S_{11} and S_{22}) and transmission (S_{12} and S_{21}) of a transverse EM wave were obtained from the VNA. According to the *S*-parameters, the reflection coefficient (*R*) and transmission coefficient (*T*) were calculated [23]: $R = |S_{11}|^2 = |S_{22}|^2$, $T = |S_{21}|^2 = |S_{12}|^2$. EMI shielding property was evaluated using *R* and *T*.

2.3. Measurement of microwave absorption property

The electromagnetic absorbing effectiveness of the sample is denoted with reflection loss (*RL*), which can be expressed as follows:

$$RL = 10 \log \frac{P_R}{P_I} (\text{dB}) \quad (1)$$

where P_I and P_R refer to incident power and the reflected power of an EM wave.

When the *RL* is below −10 dB, only 10% of the microwave energy is reflected and 90% of the microwave energy is absorbed. *RL* of the sample with a size of 180 mm × 180 mm was measured on the VNA using arc free-space method over the frequencies ranging from 8 GHz to 18 GHz. The thicknesses of the tested composites were 5 mm and 20 mm, respectively. The sample was positioned on a metal panel (180 mm × 180 mm) inserted in a heating platform, which can be heated to 800 °C on the upper surface of the metal panel. The EM signal was transmitted from the VNA through a horn antenna to the surface of the tested sample, and the other horn antenna received the reflecting signal. Then the signal was transmitted to the analyzer. The floor around the platform was covered with standard pyramidal absorbers, providing a −40 dB background level relative to the 0 dB calibration. The sample was heated in air at 20 °C/min up to certain temperature, and the value of *RL* was recorded after the temperature was stabilized for 30 min.

Table 1
Density and porosity of porous YSZ/SiC composites with different SiC content.

Sample	YSZ content (wt.%)	SiC content (wt.%)	Density (g/cm^3)	Porosity (%)
A	100	0	0.04	95
B	13.1	86.9	0.34	84.8
C	6.7	93.3	0.68	79.2
D	4.3	95.7	1.25	60.2
E	2.1	97.9	2.18	32.3

3. Results and discussion

3.1. Phase composition and microstructure of the porous composites

Fig. 1 shows the X-ray diffraction patterns of samples A, B, C, D, and E. Pure YSZ fibre felt is composed of cubic ZrO_2. After CVI, SiC matrix composed of 3C–SiC and 2H–SiC was formed in the YSZ fibre felt. Carbon peak detected at $2\theta = 26.6^\circ$ arises from the (0 0 2) plane of carbon. The SiC matrix became carbon-rich because of different reaction kinetics of the silicon and carbon-containing species, which were the intermediate decomposition products of MTS [24]. The grain sizes of 3C–SiC and 2H–SiC were 25 nm and 12 nm, respectively. The grain

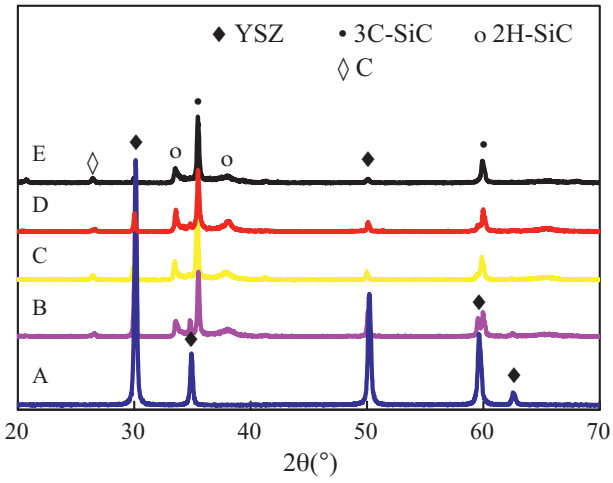

Fig. 1. XRD patterns of samples A, B, C, D, and E, revealing that SiC matrix of samples B, C, D, and E is composed of 3C–SiC and 2H–SiC.

size (D) was determined by using Scherrer equation:

$$D = \frac{k\lambda}{\beta \cos\theta} \quad (2)$$

where k is Scherrer constant (0.89), λ is wavelength of the incident ray, β is the angular line width at half maximum intensity in radians, and θ is Bragg's angle.

Fig. 2(a) displays the porous structure of YSZ fibre felt before infiltration of SiC. After CVI, there exists 84.8% open porosity in the composites with 86.9 wt.% SiC (Fig. 2(b)). The porosity of the composites decreases with the increase of SiC content, and the porosity of sample E decreases to 32.3% when the SiC content is 97.9 wt.%, as shown in Fig. 2(c). Fig. 2(d) presents the high-magnification SEM image of the fracture surface of the composites with 86.9 wt.% SiC, which shows that YSZ fibres are embedded in the dense SiC matrix layer uniformly.

3.2. Dielectric property

Fig. 3 displays the relative complex permittivity spectra and dielectric loss tangent ($\tan\delta = \varepsilon''/\varepsilon'$) of the YSZ felt and porous YSZ/SiC composites with different SiC content as a function of frequency. The mean values of relative complex permittivity (ε', ε'') and $\tan\delta$ of YSZ felt (sample A) in X-band were 1.16, 0.009 and 0.007, respectively, which all increase with increasing SiC content after CVI. When 86.9 wt.% SiC is introduced into the YSZ felt, ε', ε'' and $\tan\delta$ increase to 8.2, 10.6 and 1.31, respectively. ε', ε'' and $\tan\delta$ of the composites with 97.9 wt.% SiC reach the maximum values of 10.8, 18.2 and 1.83, respectively.

According to the theory of complex permittivity, the increase in ε' can be mainly ascribed to the bound charges, i.e., dielectric relaxation and space charge polarization effect, and the increase of ε'' can be attributed to the enhanced electric conductivity of the composites. Known from the above results, the increase in the complex permittivity with increasing SiC content is attributed to the addition of SiC in the YSZ felt.

In the microwave band, the polarizability (electronic, ionic and orientation polarization) and electric displacement of dielectric materials cannot keep up with the variation of electromagnetic field. It will appeal the phenomenon that complex permittivity decreases with increasing frequency [25], which can be observed in Fig. 3(a) and (b).

It is noteworthy that the $\tan\delta$ of the composites with 86.9 wt.% SiC enhances more than two orders over pure YSZ fibre felt, as show in Fig. 3(c), and the mean value of $\tan\delta$ reaches 1.3 in X-band. The higher dielectric loss implies that the composites possess higher attenuation ability for EM wave in X-band. The SiC matrix composed of nanocrystals in the porous YSZ/SiC composites is responsible for the higher dielectric loss. The main contributions of SiC matrix may include the grain boundaries between SiC nanocrystals, the grain boundaries between SiC nanocrytal and carbon, and the interface between YSZ and SiC, which can give rise to the space charge polarization and relaxation. The SiC nanocrystals can be repeatedly polarized under an alternating EM field, leading to a strong interfacial polarization relaxation loss and ohmic loss, and consequently to the enhancement in dielectric properties [26].

When EM wave penetrates the porous YSZ/SiC composites, the local electric field is scattered by the continuous SiC matrix

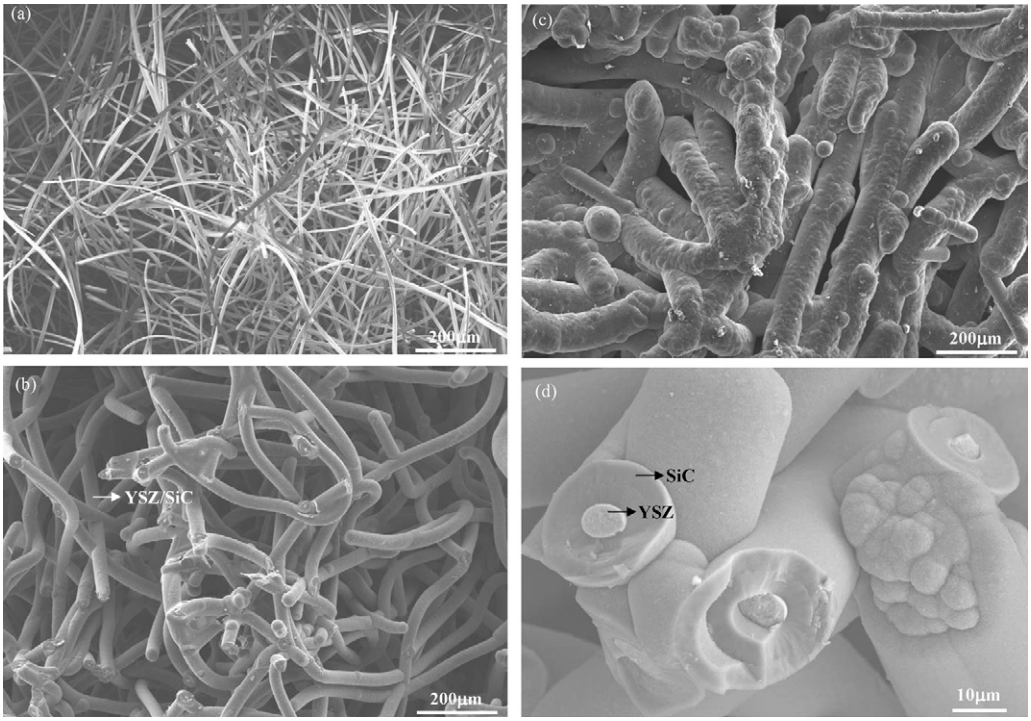

Fig. 2. Scanning electron micrographs of low-magnification surface morphologies of (a) sample A, (b) sample B, (c) sample E, and (d) high-magnification fracture surface morphology of sample B, showing the YSZ fibre embedded in SiC matrix layer.

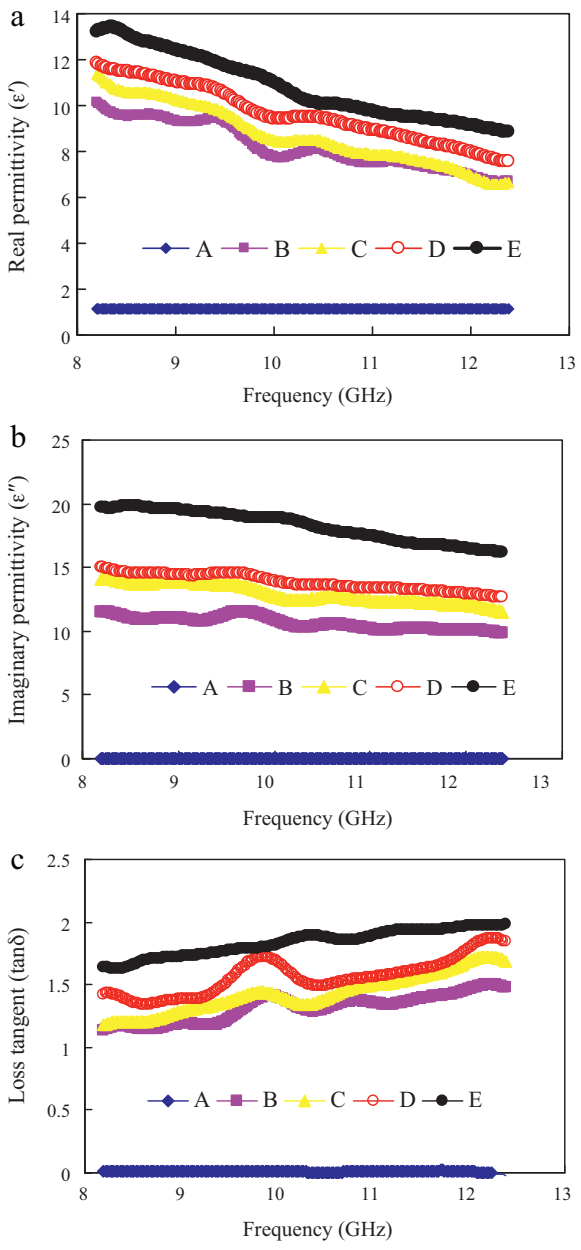

Fig. 3. Dielectric properties of porous YSZ/SiC composites: (a) ε', (b) ε'', and (c) tan δ.

layer, which propagates a much longer distance in random directions in the porous YSZ/SiC composites. As a result, induced electric current may be produced in the SiC matrix layer, and the dielectric loss is considerably increased, which can be described in the following equation [27]:

$$\tan\delta = \frac{\varepsilon''}{\varepsilon'} = \frac{\sigma}{2\pi f \varepsilon' \varepsilon_0} \tag{3}$$

where σ is electric conductivity, ε_0 is the permittivity of the free space (8.85×10^{-12} F/m), and f is frequency.

Briefly, with the increase of SiC content, σ increases, this leads to the increase of both ε'' and tan δ. The increase of σ can also lead to the improvement of the EMI shielding property of the composites.

3.3. EMI shielding property

The shielding efficiency (SE) against EMI can be defined as the ratio between the incident power (P_I) and the transmitted power (P_T) of an EM wave. The total SE of a material (SE_{Total}) is given by [28]:

$$SE_{Total} = 10\log\left(\frac{P_I}{P_T}\right)(dB) \tag{4}$$

In Schelkunoff's theory, SE_{Total} is determined by the sum of the initial reflection loss from both surfaces of the materials (loss of energy by first reflection), the absorption or penetration loss within the materials itself (loss of the energy by absorption) and the internal reflection loss at the exiting interface (loss of energy by multi-reflection). Therefore, SE_{Total} can be described as follows:

$$SE_{Total} = SE_R + SE_A + SE_M \tag{5}$$

SE_R, SE_A, and SE_M are the shielding efficiency due to reflection, absorption, and multiple reflection, respectively.

Multi-reflection refers to the reflections at various surfaces or interfaces in the materials, which requires the presence of a large surface area or interface area in the materials. When $SE_{Total} > 15$ dB, Eq. (5) is usually assumed to take the following form [4]:

$$SE_{Total} \approx SE_R + SE_A \tag{6}$$

SE_R and SE_A can be calculated according to the reflection coefficient (R) and transmission coefficient (T) by the following equations:

$$SE_R = -10\log(1-R) \tag{7}$$

$$SE_A = -10\log\left(\frac{T}{1-R}\right) \tag{8}$$

Generally, the increase of SE_R represents increasing impedance mismatch between air and materials when frequency varies, and the increase of SE_A represents increasing attenuation of EM energy in the materials. Therefore, the materials with low SE_R and high SE_A are expected for microwave absorption.

As shown in Fig. 4(a), the mean value of SE_{Total} of pure YSZ felt is only 0.069 dB in X-band, implying that pure YSZ felt is a microwave-transparent material. When 86.9 wt.% SiC is introduced into the porous YSZ felt, SE_{Total} drastically increases to 16.2 dB, which shows good EMI shielding property. SE_{Total} increases with increasing SiC content, which reaches 20.3 dB when SiC content is 97.9 wt.%. The enhancement of the EMI SE is mainly attributed to the formation of continuous interlocked SiC matrix layer around the YSZ fibres, which acts as the conductive networks, as confirmed by SEM image in Fig. 2(d). The SiC matrix layer will interact with the incident radiation and lead to a higher EMI SE. The target value of the EMI SE needed for commercial applications is around 20 dB. Hence the composites with

97.9 wt.% SiC can be used as light-weight EMI shielding materials.

The porous YSZ/SiC composites show high SE_A and low SE_R, implying absorption is the primary EMI shielding mechanism. SE_R of the composites decreases with increasing frequency (Fig. 4(b)), but SE_A increases (Fig. 4(c)). The above results are consistent with the following equations, which show expressions of SE_R and SE_A as functions of frequency [28]:

$$SE_R = 39.5 + 10\log\frac{\sigma}{2\pi f\mu} \quad (9)$$

$$SE_A = 8.7d\sqrt{\pi f\mu\sigma} \quad (10)$$

where μ is permeability, and d is specimen thickness.

The increase of SiC content leads to the increase of σ, so both SE_R and SE_A increase with increasing SiC content according to Eqs. (9) and (10), which is consistent with Fig. 4. Specific EMI shielding efficiency (EMI SE divided by density) of the composites with 86.9 wt.% SiC is 47.6 dB cm^3/g, much higher than that of typical metals, 10 dB cm^3/g for copper [29], so the composite is attractive for aerospace applications. Since the composites with 86.9 wt.% SiC has the lowest SE_R due to the good EM wave impedance with air and high loss tangent (>1), the good microwave-absorbing properties are expected.

3.4. Microwave absorption property

When the sample thickness is 5 mm (Fig. 5(a)), the measured *RL* of sample B at room temperature (B-RT) over the frequencies ranging from 8 GHz to 18 GHz is smaller than −6.5 dB and the bandwidth of B-RT below −10 dB is 5 GHz. A maximum absorbing peak with minimum *RL* of −26.6 dB appears at 16.5 GHz. It is worthwhile to note that the bandwidth below −10 dB increases to 5.3 GHz, 5.7 GHz and 5.9 GHz at 300 °C, 600 °C and 800 °C, respectively. The values of tan δ of SiC and ZrO_2 increase with temperature [10], so the EM wave absorption of the composites at higher temperature exhibits broader bandwidth. When the sample thickness is 20 mm (Fig. 5(b)), the EM wave absorbing property is even better. The

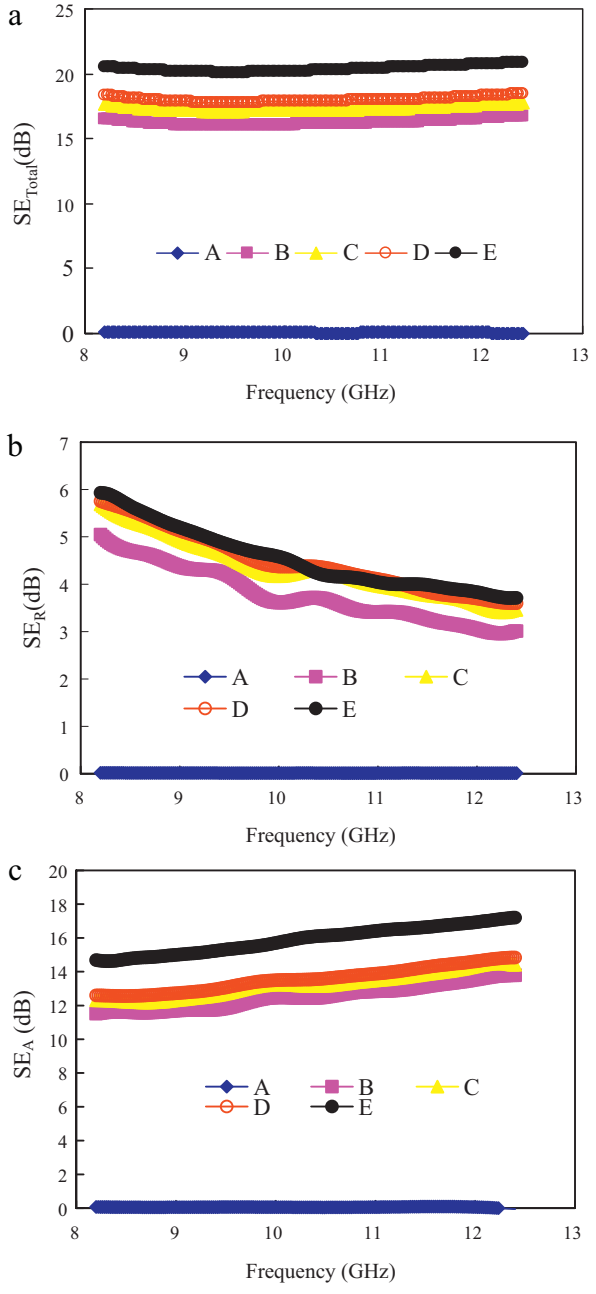

Fig. 4. Dependence of EMI shielding efficiency of the porous composites with different SiC content on frequency: (a) SE_{Total}, (b) SE_R, and (c) SE_A.

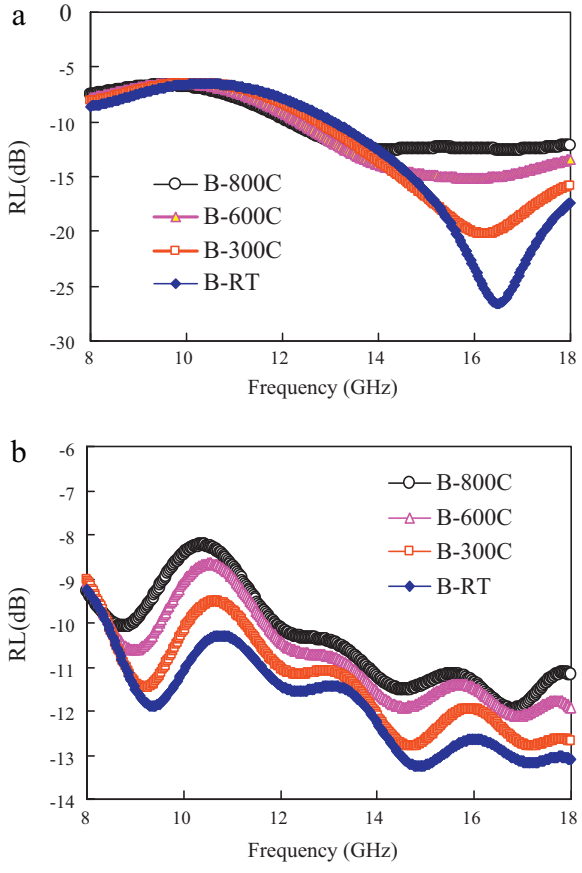

Fig. 5. Reflection loss at different temperature as a function of frequency for sample B with different thickness: (a) 5 mm and (b) 20 mm.

measured *RL* of sample B at room temperature over the frequencies ranging from 8 GHz to 18 GHz is smaller than −9.2 dB, and the bandwidth below −10 dB is 9.6 GHz.

When the sample thickness (t) is approximately a quarter of the propagating wavelength (λ) multiplied by an odd number, i.e. $t = n\lambda/4$ ($n = 1, 3, 5, 7, 9, \ldots$), the cancellation of the incident and reflected waves at the air–material interface occurs. Thus, a maximum absorbing peak corresponding to the minimum *RL* of the EM wave appears. The value of λ in the porous YSZ/SiC composites can be calculated according to Eq. (11) [30]:

$$\lambda = \frac{\lambda_0}{\sqrt{|\varepsilon||\mu|}} \tag{11}$$

where λ_0 is the wavelength in free space, $|\varepsilon|$ and $|\mu|$ are the moduli of ε and μ of the porous YSZ/SiC composite, respectively. μ is taken as 1 because of the negligible magnetic properties of YSZ/SiC composites.

Taking the sample with a thickness of 20 mm for example, by putting the values of $|\varepsilon|$ and $|\mu|$ into Eq. (11), the values of λ in sample B at 9.2 GHz and 12.4 GHz are 8.64 mm and 7.02 mm, respectively. Therefore, the values of $\lambda/4$ multiplied by 9 and 11, respectively, are close to 20 mm. As a result, there are cancellations of the incident and reflected waves on the sample surface at 9.2 GHz and 12.4 GHz, leading to the maximum EM absorbing peaks, as shown in Fig. 5(b).

4. Conclusions

SiC was infiltrated into yttria-stabilized zirconia (YSZ) felt by chemical vapor infiltration (CVI), and continuous SiC matrix layer was formed around the YSZ fibre. The increase of SiC content leads to the increase of relative complex permittivity of the porous YSZ/SiC composites. The considerable increases of electromagnetic interference shielding and microwave absorption properties are attributed to the formation of continuous SiC matrix layer composed of SiC nanocrystals, which is beneficial for the production of induced electric current and the increase of dielectric loss tangent. Since the porous YSZ/SiC composite has high dielectric loss tangent, it exhibits good EM wave absorbing ability not only at room temperature but also at high temperature. Therefore, the composites could be used as an effective lightweight microwave absorbing material at high temperature up to 800 °C.

Acknowledgement

This work was supported by the fund of the State Key Laboratory of Solidification Processing in Northwestern Polytechnical University (No. KB200920).

References

[1] D.D.L. Chung, Electromagnetic interference shielding effectiveness of carbon materials, Carbon 39 (2001) 279–285.
[2] M.S. Cao, W.L. Song, Z.L. Hou, B. Wen, J. Yuan, The effects of temperature and frequency on the dielectric properties, electromagnetic interference shielding and microwave-absorption of short carbon fiber/silica composites, Carbon 48 (2010) 788–796.
[3] C. Wang, X.J. Han, P. Xu, X.L. Zhang, Y.C. Du, S.R. Hu, et al., The electromagnetic property of chemically reduced graphene oxide and its application as microwave absorbing material, Appl. Phys. Lett. 98 (2011), 072906–072906-3.
[4] J. Wang, C. Xiang, Q. Liu, Y. Pan, J. Guo, Ordered mesoporous carbon/fused silica composites, Adv. Funct. Mater. 18 (2008) 2995–3002.
[5] S. Shi, L. Zhang, J. Li, Ti_3SiC_2 material: an application for electromagnetic interference shielding, Appl. Phys. Lett. 93 (2008), 172903–172903-3.
[6] G. Bantsis, C. Sikalidis, M. Betsiou, T. Yioultsis, T. Xenos, Electromagnetic absorption, reflection and interference shielding in X-band frequency range of low cost ceramic building bricks and sandwich type ceramic tiles using mill scale waste as an admixture, Ceram. Int. 37 (2011) 3535–3545.
[7] C. Xiang, Y. Pan, J. Guo, Electromagnetic interference shielding effectiveness of multiwalled carbon nanotube reinforced fused silica composites, Ceram. Int. 33 (2007) 1293–1297.
[8] K. Li, C. Wang, H. Li, X. Li, H. Ouyang, J. Wei, Effect of chemical vapor deposition treatment of carbon fibers on the reflectivity of carbon fiber-reinforced cement-based composites, Comp. Sci. Technol. 68 (2008) 1105–1114.
[9] T. Razzaq, J.M. Kremsner, C.O. Kappe, Investigating the existence of nonthermal/specific microwave effects using silicon carbide heating elements as power modulators, J. Org. Chem. 73 (2008) 6321–6329.
[10] M. Gupta, E.W.W. Leong, Microwaves and Metals, John Wiley, Singapore, 2007.
[11] D. Zhao, F. Luo, W. Zhou, Microwave absorbing property and complex permittivity of nano SiC particles doped with nitrogen, J. Alloys Compd. 490 (2010) 190–194.
[12] R. Wongmaneerung, P. Singjai, R. Yimnirun, S. Ananta, Effects of SiC nanofibers addition on microstructure and dielectric properties of lead titanate ceramics, J. Alloys Compd. 475 (2009) 456–462.
[13] H. Zhang, J. Zhang, H. Zhang, Electromagnetic properties of silicon carbide foams and their composites with silicon dioxide as matrix in X-band, Composites Part A 38 (2007) 602–608.
[14] X. Yu, W. Zhou, F. Luo, W. Zheng, D. Zhu, Effect of fabrication atmosphere on dielectric properties of SiC/SiC composites, J. Alloys Compd. 479 (2009) L1–L3.
[15] J.E. Atwater, R.R. Wheeler, Complex permittivities and dielectric relaxation of granular activated carbons at microwave frequencies between 0.2 and 26 GHz, Carbon 41 (2003) 1801–1807.
[16] X.L. Shi, M.S. Cao, X.Y. Fang, J. Yuan, Y.Q. Kang, W.L. Song, High-temperature dielectric properties and enhanced temperature-response attenuation of β-MnO_2 nanorods, Appl. Phys. Lett. 93 (2008) 223112.
[17] T.A. Baeraky, Microwave measurements of dielectric properties of zinc oxide at high temperature, Egypt. J. Solids 30 (2007) 13–18.
[18] W. Song, M. Cao, Z. Hou, J. Yuan, X. Fang, High-temperature microwave absorption and evolutionary behavior of multiwalled carbon nanotube nanocomposite, Scr. Mater. 61 (2009) 201–204.
[19] X. Zhang, B. Lin, Y. Ling, Y. Dong, D. Fang, G. Meng, X. Liu, Highly permeable porous YSZ hollow fiber membrane prepared using ethanol as external coagulant, J. Alloys Compd. 494 (2010) 366–371.
[20] S. Heiroth, R. Ghisleni, T. Lippert, J. Michler, A. Wokaun, Optical and mechanical properties of amorphous and crystalline yttria-stabilized zirconia thin films prepared by pulsed laser deposition, Acta Mater. 59 (2011) 2330–2340.
[21] J. Battat, J.P. Calame, Analysis of the complex dielectric permittivity behavior of porous Al_2O_3–SiC composites in the 1 MHz to 18 GHz frequency range, J. Mater. Res. 22 (2007) 3292–3302.
[22] X. Li, L. Zhang, X. Yin, Z. Yu, Mechanical and dielectric properties of porous Si_3N_4–SiC(BN) ceramic, J. Alloys Compd. 490 (2010) L40.
[23] Y.K. Hong, C.Y. Lee, C.K. Jeong, J.H. Sim, K. Kim, J. Joo, Electromagnetic interference shielding characteristics of fabric complexes coated with conductive polypyrrole and thermally evaporated Ag, Curr. Appl. Phys. 1 (2001) 439–442.
[24] S.H. Mousavipour, V. Saheb, S. Ramezani, Kinetics and mechanism of pyrolysis of methyltrichlorosilane, J. Phys. Chem. A 108 (2004) 1946–1952.

[25] G. Wang, X. Chen, Y. Duan, S. Liu, Electromagnetic properties of carbon black and barium titanate composite materials, J. Alloys Compd. 454 (2008) 340–346.
[26] H. Zhu, Y. Bai, R. Liu, N. Lun, Y. Qi, F. Han, et al., Microwave absorption properties of MWCNT–SiC composites synthesized via a low temperature induced reaction, AIP Adv. 1 (2011) 032140.
[27] W.D. Kingery, H.K. Bowen, D.R. Uhlmann, Introduction to Ceramics, John Wiley and Sons, New York, 1976.
[28] M.H. Al-Saleh, U. Sundararaj, Electromagnetic interference shielding mechanisms of CNT/polymer composites, Carbon 47 (2009) 1738–1746.
[29] X. Shui, D.D.L. Chung, Nickel filament polymer–matrix composites with low surface impedance and high electromagnetic interference shielding effectiveness, J. Electron. Mater. 26 (1997) 28–934.
[30] A.N. Yusoff, M.H. Abdullah, S.H. Ahmad, S.F. Jusoh, A.A. Mansor, S.A.A. Hamid, Electromagnetic and absorption properties of some microwave absorbers, J. Appl. Phys. 92 (2002) 876–882.